^{2}H NMR Detection of Transmembrane Potential-Driven Tetraphenylphosphonium Transbilayer Redistribution†

Carla M. Franzin and Peter M. Macdonald*

Department of Chemistry and Erindale College, University of Toronto, Toronto, Ontario, Canada

Received May 30, 1995; Revised Manuscript Received September 11, 1995⊗

ABSTRACT: ^{2}H NMR of specifically choline-deuterated phosphatidylcholine incorporated into giant unilamellar vesicles (GUVs), composed of 1−palmitoyl-2-oleoyl-*sn*-glycero-3-phosphocholine (POPC) plus 1−palmitoyl-2-oleoyl-*sn*-glycero-3-phosphoglycerol (POPG) plus cholesterol (CHOL), was shown to detect a transmembrane potential-driven redistribution of the potential-sensitive, surface- binding dye tetraphenylphosphonium (TPP^+) across the GUV lipid bilayer. The method is based on resolving differences in the surface charge at the inner versus the outer monolayer of the vesicle's bilayer using the so-called ^{2}H NMR "molecular voltmeter" technique. A mathematical model to describe the ^{2}H NMR results was derived by combining the Nernst, Boltzmann, Langmuir, and Gouy- Chapman equations with the established sensitivity of deuterium quadrupolar splittings from choline- deuterated POPC to surface electrostatic charge effects. This model identified experimental factors likely to yield enhanced sensitivity and resolution of the inner versus outer monolayer surface charges via ^{2}H NMR. The predictions of the model were then confirmed experimentally. The improvement in resolution resulting from these studies removes a major hindrance to the general exploitation of ^{2}H NMR for monitoring transbilayer surface charge asymmetries.

Solid state deuterium (^{2}H) nuclear magnetic resonance (NMR) studies of phospholipid bilayers indicate that bilayer surface charges induce a conformational change in the head group of certain phospholipids (Sixl & Watts, 1983; Seelig et al., 1987; Roux et al., 1989; Scherer & Seelig, 1989; de Kroon et al., 1991a; Marassi & Macdonald, 1991). In phosphatidylcholine (PC), the P^--N^+ dipole of the choline head group appears to realign under the influence of a surface electrical field (Akutsu & Seelig, 1981; Roux et al., 1989; Scherer & Seelig, 1989; Macdonald et al., 1991; Marassi & Macdonald, 1992). If the PC head group is specifically deuterated, the conformational change alters the measured ^{2}H NMR quadrupolar splittings.

This so-called ^{2}H NMR "molecular voltmeter" behavior of PC can be exploited to study a variety of membrane surface charge-associated phenomena, including the surface binding of ions (Altenbach & Seelig, 1985; Roux & Bloom, 1990; Rydall & Macdonald, 1992), anaesthetics (Boulanger et al., 1981; Seelig et al., 1988), and peptides (Kuchinka & Seelig, 1989; Demsey et al., 1989; Roux et al., 1989; Beschiaschvili & Seelig, 1991), the pK_a of surface-bound ionizable groups (Watts & Poile, 1986; Lau & Macdonald, 1995), and the lateral phase separation of lipid mixtures (Marassi et al., 1993a).

Almost all such studies to date have used multilamellar vesicles (MLVs) as model membranes. Many fundamental membrane processes can only be modeled, however, in unilamellar vesicles. A particular example is the transmembrane potential, $\Delta\Psi_{tm}$, which drives a multitude of biomembrane functions such as ion channel function, signal transduction, and the insertion and translocation of proteins (Davidson et al., 1984; Caterall et al., 1986; Alberts et al., 1989). Unilamellar vesicles are unique in that, unlike MLVs, the aqueous solution is divided into two, and only two, discrete compartments: the intra- and the extravesicular solutions. For the purposes of ^{2}H NMR, it is critical that the lipids of a unilamellar vesicle are divided into two, and only two, discrete populations: those of the inner and the outer monolayers of the vesicle bilayer.

Recently, we demonstrated that differences in the surface charge at the inner versus the outer monolayer of the lipid bilayers of giant unilamellar vesicles (GUVs) can be resolved using the ^{2}H NMR molecular voltmeter technique (Marassi et al., 1993b). This capability permits a new application of ^{2}H NMR in lipid bilayer studies, probing for transbilayer surface charge asymmetries. These might originate with a transmembrane electrical potential or an asymmetry of lipid distribution, ion location, or protein configuration. An innovative application of this ^{2}H NMR technique was described recently by de Kruijff and coworkers (Leenhouts et al., 1993), who showed convincingly that in GUVs ^{2}H NMR detects the presence of $\Delta\Psi_{tm}$ indirectly through its effects on the transbilayer distribution of the potential-sensitive, surface-binding dye tetraphenylphosphonium (TPP^+). This experiment constitutes an archetype of the entire ^{2}H NMR strategy for resolving transbilayer surface charge asymmetries. Unfortunately, the resolution and sensitivity currently achievable with ^{2}H NMR measurements in GUVs is rather limited, to the point of preventing its general exploitation for such studies.

The purpose of this report is to describe a systematic approach to enhancing resolution and sensitivity in ^{2}H NMR measurements of transbilayer surface charge asymmetries. First, we propose a model of the response of the ^{2}H NMR

† This work was supported by an Operating Grant (P.M.M.) and a Graduate Scholarship (C.M.F.) from the National Science and Engineering Research Council (NSERC) of Canada.

* To whom correspondence should be addressed. Telephone: 905-828-3805. Fax: 905-828-5425. E-mail: pmacdona@credit.erin.utoronto.ca.

⊗ Abstract published in *Advance ACS Abstracts,* December 15, 1995.

0006-2960/96/0435-851$12.00/0

quadrupolar splittings of head group-deuterated PC for the case of TPP^+ binding to unilamellar lipid bilayer vesicles in the presence of a transmembrane potential. This allows us to identify those factors influencing the quadrupolar splitting which are subject to experimental control and to predict their interplay. Second, we demonstrate that the predictions of the model are confirmed experimentally in GUVs. This permits optimization of experimental conditions, leading to profound improvements in the sensitivity and resolution of transbilayer surface charge asymmetry measurements via the ^2H NMR molecular voltmeter technique. It likewise provides some perspective on the ultimate limitations particular to ^2H NMR.

MATERIALS AND METHODS

Materials. Nondeuterated lipids were purchased from Avanti Polar Lipids (Alabaster, AL). *n*-Octyl β-glucopyranoside (OG), valinomycin, and Safranin O were obtained from Sigma (St. Louis, MO). 4-(2-Hydroxyethyl)piperazine-1-ethanesulfonic acid (HEPES) was purchased from BDH (Toronto, ON). Tetraphenylphosphonium chloride (TPP^+) and 2,3,4−triisopropylbenzenesulfonyl chloride (TPS) were purchased from Aldrich (Milwaukee, WI). Cholesterol (CHOL) was purchased from Fisher (Ottawa, ON) and recrystallized from ethanol prior to use. Choline chloride was obtained from Fluka (Buchs, Switzerland).

Synthesis of Deuterated Lipids. 1-Palmitoyl-2-oleoyl-*sn*-glycero-3-phosphocholine (POPC) was selectively deuterated at the α or β choline methylene segment by a modification of the methods of Harbisson and Griffin (1984) and Aloy and Rabout (1913). The structure of the phosphocholine head group is as shown below:

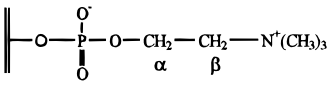

Briefly, POPC-α-d_2 and POPC-β-d_2 were prepared by coupling the corresponding deuterated cholines to 1-palmitoyl-2-oleoyl-*sn*-glycero-3-phosphate (POPA) in pyridine, using TPS (recrystallized from *n*-pentane) as the condensing agent (Aneja et al., 1970). The deuterated phosphatidylcholines were purified by chromatography on an Amberlite mixed-bed ion exchanger (BDH, Toronto, ON), followed by chromatography on silica gel and/or CM-52, the latter as described by Comfurius and Zwaal (1977). Thin layer chromatography and proton and deuterium NMR were used to confirm the purity of the synthesized lipids.

GUV Preparation. Giant unilamellar vesicles were prepared following a modification of the procedure of Marassi et al. (1993b). Deuterated POPC (20 mg) was mixed with POPG (1-palmitoyl-2−oleoyl-*sn*-glycero-3-phosphoglycerol) and cholesterol (all dissolved in chloroform) in the desired molar ratio. Solvent was removed under a stream of argon gas, followed by several hours under vacuum over calcium chloride. The dried lipids were dispersed in 750 μL of potassium sulfate buffer [150 mM K_2SO_4 and 10 mM HEPES (pH 7.0)] plus OG in a detergent:lipid molar ratio of 12:1. The mixture was vortexed and warmed to 40 °C until a clear micellar solution was formed. The detergent/lipid mixture was injected into the dialysis cell of a MiniLipoPrep dialyzer (Avestin, Ottawa, ON) and dialyzed through a cellulose membrane (molecular weight cutoff of 5000, Diachema, Switzerland) against 1 L of K_2SO_4 buffer. Dialysis proceeded for 48 h, with four buffer changes.

Generation of Transmembrane Potential. The external potassium buffer of the GUVs was replaced with a buffer containing 225 mM choline chloride and 10 mM HEPES (pH 7.0) by passing the vesicles through a Sephadex G-10 column (Sigma, St. Louis, MO) equilibrated in the same choline chloride buffer. The external buffer-exchanged vesicles were then concentrated to about 1.4 mL using a Centricon-10 microconcentrator (Amicon, Oakville, ON). A transmembrane potential was generated using valinomycin (1 mg/mL in ethanol) in a $1:10^4$ molar ratio with respect to phospholipid. The presence of the membrane potential was established spectroscopically using the cationic potential-sensitive probe Safranin O on a 10 μL sample of vesicles diluted into the same choline chloride buffer (Åkerman & Saris, 1976).

Deuterium NMR Measurements. ^2H NMR spectra were recorded on a Chemagnetics CMX300 NMR spectrometer operating at 45.98 MHz, using a Doty 402 Wideline Double Resonance probe. The quadrupolar echo pulse sequence (Davis et al., 1976) was employed using quadrature detection with complete phase cycling of the pulse pairs and a 90° pulse length of 7.5 μs, an interpulse delay of 40 μs after the first 90° pulse, a recycle delay of 100 ms, a spectral width of 250 kHz, and a 2*k* data size. All spectra were recorded at room temperature.

RESULTS AND DISCUSSION

A Model of the ^2H NMR Response to a $\Delta\Psi_{tm}$-Driven TPP^+ Redistribution. The immediate goal is to define mathematically the relationship between the transmembrane potential and the ^2H NMR quadrupolar splitting as mediated by a potential-sensitive ion capable of redistributing across a membrane in response to such a transmembrane potential. The ion also binds to a lipid bilayer surface and in so doing induces a surface electrostatic potential sensed by the molecular voltmeter. Our intention is to identify the variables which most influence the ^2H NMR response, and which are under experimental control, so that we can predict conditions under which resolution of differences between the inner and outer monolayers will be optimal. Our starting point is the model of Cafiso and Hubbell (1978), and later Rottenberg (1984), who used the Nernst equation to describe the redistribution of TPP^+ across lipid vesicles in the presence of a transmembrane potential $\Delta\Psi_{tm}$:

$$\Delta\Psi_{tm} = -\frac{RT}{F}\ln\frac{[TPP^+]^i}{[TPP^+]^o} \qquad (1)$$

where R is the gas constant, F is the Faraday constant, T is the absolute temperature, and the superscipts i and o refer to the inner and outer vesicular solutions, respectively. For given extravesicular and intravesicular volumes, V^o and V^i, the concentration of TPP^+ in the internal bulk solution, $[TPP^+]^i$, is obtained as follows:

$$\frac{[TPP^+]^i}{[TPP^+]^t} = \left(1+\frac{V^o}{V^i}\right)\left(1+\frac{V^o}{V^i}e^{+\Phi_{tm}}\right)^{-1} \qquad (2)$$

and similarly for the concentration of TPP^+ in the external bulk solution, $[TPP^+]^o$:

$$\frac{[TPP^+]^o}{[TPP^+]^t} = \left(1 + \frac{V^o}{V^i}\right)\left(1 + \frac{V^o}{V^i}e^{-\Phi_{tm}}\right)^{-1} \quad (3)$$

where $[TPP^+]^t$ is the overall molar concentration of TPP$^+$ with respect to global vesicle solution and $\Phi_{tm} = \Delta\Psi_{tm}\,F/RT$. The volume occupied by the bilayer is considered to be negligible.

TPP$^+$ binds to lipid membranes at sites located near the membrane surface (Ketterer et al., 1971) and in so doing creates a positive surface potential, Ψ_s. Cafiso and Hubbell (1978) and Rottenberg (1984) considered the case of low concentrations of TPP$^+$ (1 mM) equilibrating across neutral PC bilayers. Hence, it could reasonably be assumed that TPP$^+$ binding is quantitative. In the present case, we are interested, of necessity, in a higher range of TPP$^+$ concentrations, so that the equilibrium aspects of TPP$^+$ binding have to be considered. Moreover, we wish to consider cases where the initial membrane surface charge might not be zero.

The TPP$^+$ concentration of relevance for its surface binding equilibrium is that in the solution immediately adjacent to the inner or outer membrane surface, $[TPP^+]^{i/o}_m$, which is related to the bulk TPP$^+$ concentration in the inner or outer vesicle solution, $[TPP^+]^{i/o}$, through the membrane surface potential, $\Psi_s^{i/o}$, according to the Boltzmann equation:

$$[TPP^+]_m^{i/o} = [TPP^+]^{i/o}\exp\left(\frac{-F\Psi_s^{i/o}}{RT}\right) \quad (4)$$

The binding equilibrium between TPP$^+$ in the aqueous solution adjacent to the membrane surface and membrane surface sites is described via a Langmuir adsorption isotherm:

$$K[TPP^+]_m = \frac{\theta}{(1-\theta)} = \frac{nX_{TPP}}{(1 - nX_{TPP})} \quad (5)$$

where θ is the fraction of sites occupied, K is the association constant, X_{TPP} is the mole fraction of lipids bound to TPP$^+$, and n is the number of lipids forming a binding site. For different multiply charged species, the surface charge density, σ, is related directly to the mole fraction of a particular charged species present at the membrane surface according to

$$\sigma = \frac{e\sum_j z_j X_j}{\sum_j X_j S_j} \quad (6)$$

where e is the elementary charge of an electron, z_j is the valence of a particular species, X_j is the mole fraction of a particular lipid, and S_j is the surface area of that lipid. The surface charge density produces a surface potential which may be estimated using the Graham equation:

$$\sigma^2 = 2000\epsilon_r\epsilon_o RT\sum_k C_k\left[\exp\left[\frac{(-z_k F\Psi_s)}{RT}\right] - 1\right] \quad (7)$$

where ϵ_r is the dielectric constant of water, ϵ_o is the permitivity of free space, and C_k is the concentration of the kth electrolyte in the bulk phase. The mole fraction of lipids bound to TPP$^+$ at either the inner or the outer monolayer surface of a lipid bilayer is then obtained by combining eqs 4 and 5 with either 2 or 3:

$$X^o_{TPP} = n^{-1}(1 + B/A)^{-1} \quad X^i_{TPP} = n^{-1}(1 + C/A)^{-1} \quad (8)$$

$$A = K[TPP^+]^t\left(1 + \frac{V^o}{V^i}\right)$$

$$B = e^{+\Phi_s^o}\left(1 + \frac{V^o}{V^i}e^{-\Phi_{tm}}\right) \quad (9)$$

$$C = e^{+\Phi_s^i}\left(1 + \frac{V^o}{V^i}e^{+\Phi_{tm}}\right)$$

where $\Phi_s^{i/o} = \Psi_s^{i/o}F/RT$.

At low surface charge densities, the deuterium quadrupolar splitting in the presence of a given charged species j, $\Delta\nu_j$, is approximately a linear function of the mole fraction of that species according to

$$\Delta\nu_j = \Delta\nu_o + m_j X_j \quad (10)$$

where $\Delta\nu_o$ is the deuterium quadrupolar splitting for a neutral surface and m_j is the slope of the linear function describing the dependence of the quadrupolar splitting on the level of charge. When two charged species, j and k, are present at the membrane surface simultaneously, the measured quadrupolar splitting, $\Delta\nu_{jk}$, is perturbed from the value measured for a neutral membrane surface to a degree which may be predicted from knowledge of the individual perturbations due to the two species separately (Marassi & Macdonald, 1992), as illustrated in eq 11.

$$\begin{aligned}(\Delta\nu_{jk} - \Delta\nu_o) &= (\Delta\nu_j - \Delta\nu_o) + (\Delta\nu_k - \Delta\nu_o)\\ &= m_j X_j + m_k X_k\end{aligned} \quad (11)$$

For the case that j equals TPP$^+$ and k equals some charged species which does not redistribute with the transmembrane potential (e.g. POPG), the difference in the quadrupolar splitting between the inner and outer monolayer of the vesicle bilayer is then readily shown to equal

$$(\Delta\nu^o_{jk} - \Delta\nu^i_{jk}) = \frac{m_j}{n}[(1 + B/A)^{-1} - (1 + C/A)^{-1}] \quad (12)$$

Equations 11 and 12 indicate that four experimental variables should have a direct impact on the size of the quadrupolar splittings; these are the ratio of the inner to outer vesicular volumes, V^o/V^i, the transmembrane potential, $\Delta\Psi_{tm}$, the initial surface potentials at the inner and outer vesicular surfaces as dictated by the mole fraction of a negatively charged lipid such as phosphatidylglycerol, X_{PG}, and, finally, the overall TPP$^+$ concentration, $[TPP^+]^t$. Other factors, such as the membrane association constant, K, for the ligand under consideration or the ^{2}H NMR sensitivity parameter, m_j, certainly play a role but are not under experimental control.

Predictions of the Model. The procedure for obtaining a prediction for a quadrupolar splitting involves first selecting the desired values of the experimental variables V^o/V^i, $\Delta\Psi_{tm}$, X_{PG}, and $[TPP^+]^t$, in addition to making appropriate choices for the constants K, m_j, m_k, and n. Next, using eqs 2 and 3,

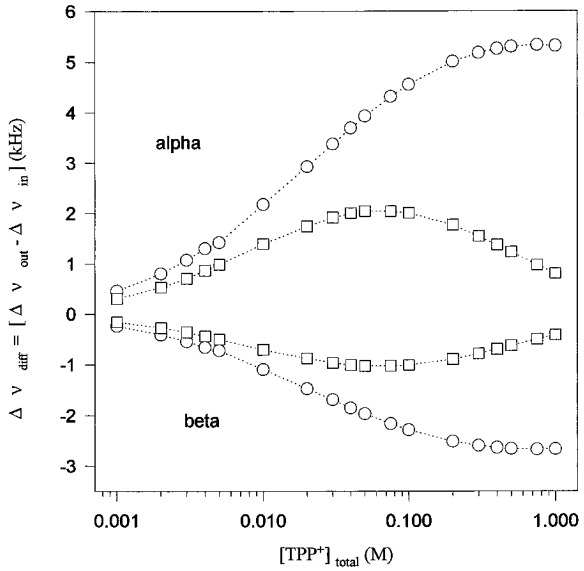

FIGURE 1: Model predictions of the effect of different $\Delta\Psi_{tm}$ values on the difference between the ^{2}H NMR quadrupolar splitting from the inner versus the outer monolayer, $\Delta\nu_{diff}$, for POPC-α-d_2 and POPC-β-d_2, in GUVs composed of POPC/POPG/CHOL (70/10/20) with $V^o/V^i = 1$: circles, $\Delta\Psi_{tm} = -200$ mV; and squares, $\Delta\Psi_{tm} = -50$ mV.

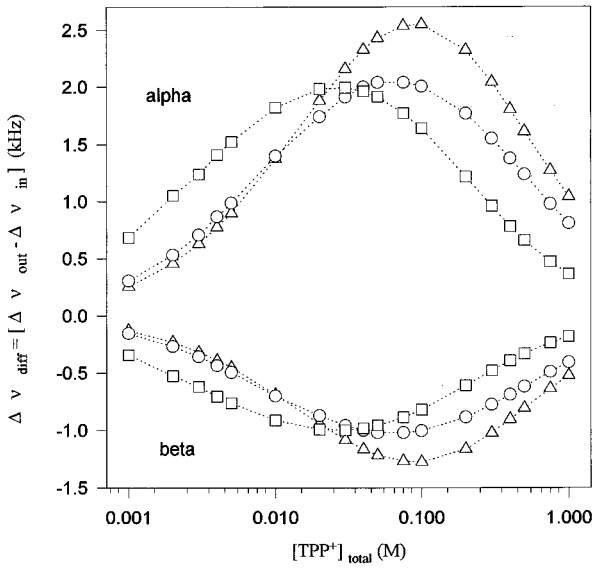

FIGURE 2: Model predictions of the effects of changing the ratio of the extra- to intravesicular volume, V^o/V^i, on the difference between the ^{2}H NMR quadrupolar splittings from the inner versus the outer monolayer, $\Delta\nu_{diff}$, for POPC-α-d_2 and POPC-β-d_2 , in GUVs composed of POPC/POPG/CHOL (70/10/20) and having $\Delta\Psi_{tm} = -50$ mV: triangles, $V^o/V^i = 0.1$; circles, $V^o/V^i = 1$; and squares, $V^o/V^i = 10$.

the bulk concentrations of TPP^+ on the inside, $[TPP^+]^i$, and the outside, of the vesicle are calculated. Subsequently, one makes an initial "guess" at the mole fraction of lipids bound to TPP^+, X_{TPP}, for either the inner or the outer monolayer. The quality of this guess is judged by comparison of the surface electrostatic charge, σ, calculated according to eq 6, with that calculated from the Graham equation (eq 7). The value for the surface potential, Ψ_s, used in eq 7 is obtained from the Boltzmann equation (eq 4) for the particular $[TPP^+]_m$ implied by the choice of X_{TPP} after substitution into the Langmuir adsorption isotherm equation (eq 5). When the values of the surface charge density calculated by these two routes agree with one another, the choice of X_{TPP} is taken to be correct. The ^{2}H NMR quadrupolar splitting is then obtained using eq 11 for the inner or outer vesicle surfaces separately or as the difference between the two using eq 12.

Figures 1−3 illustrate the manner in which the difference in the quadrupolar splittings between the inner and outer vesicle surfaces, $\Delta\nu_{diff} = (\Delta\nu^o - \Delta\nu^i)$, is predicted to behave as a function of the overall TPP^+ concentration, $[TPP^+]^t$, for different values of the other three variables $\Delta\Psi_{tm}$, V^o/V^i, and X_{PG}. All calculations are for GUVs composed of POPC/POPG/CHOL with the mole fraction of cholesterol held constant at 20%. This choice reflects the composition we commonly employ in our ^{2}H NMR measurements on GUVs. It is assumed that POPC and POPG occupy roughly the same surface area of 68 Å^2 (Altenbach & Seelig, 1984), whereas cholesterol occupies a surface area of approximately 50 Å^2 (Yeagle, 1988). The TPP^+ association constant is taken to be 21 M^{-1}, while a TPP^+ binding site is assumed to consist of 8.3 lipids on average (Altenbach & Seelig, 1985). It is assumed that the presence of POPG or CHOL has no influence on these parameters. For TPP^+, the sensitivity of the ^{2}H NMR quadrupolar splittings, m_{TPP}, has been reported to equal −40 kHz/mol for POPC-α-d_2 and +20 kHz/mol for POPC-β-d_2 (Altenbach & Seelig, 1985). For POPG, the sensitivity of the ^{2}H NMR quadrupolar splittings, m_{PG}, has been reported to equal +10 kHz/mol for POPC-α-d_2 and −10 kHz/mol for POPC-β-d_2 (Macdonald et al., 1991).

Figure 1 illustrates the impact of the size of $\Delta\Psi_{tm}$ on $\Delta\nu_{diff}$ for the case $V^o = V^i$, and $X_{PG} = 0.1$, i.e. GUVs composed of POPC/POPG/CHOL (70/10/20). For the two transmembrane potentials, −50 and −200 mV (negative with respect to the vesicle interior), the TPP^+ concentration in the intravesicular solution always exceeds that of the extravesicular solution. Consequently, the amount of TPP^+ bound to the inner monolayer always exceeds the amount bound to the outer monolayer. Thus, the quadrupolar splitting at the inner surface is most perturbed from its initial value so that $\Delta\nu_{diff}$ tends to increase in magnitude, regardless of the deuteron-labeling position. As expected, a greater $\Delta\Psi_{tm}$ yields a greater difference in quadrupolar splitting for a given total concentration of TPP^+. However, there is an optimal TPP^+ concentration above which $\Delta\nu_{diff}$ decreases in magnitude rather than increases. At higher TPP^+ concentrations, the level of TPP^+ binding at the outer vesicle surface eventually catches up with the level of TPP^+ binding at the inner vesicle surface. Also worthy of mention is the fact that POPC-α-d_2 is predicted to produce greater values of $\Delta\nu_{diff}$ than POPC-β-d_2, simply because the molecular voltmeter responds with greater sensitivity at the α versus β deutero-labeling position in the choline head group.

Figure 2 illustrates the predicted effects of varying the ratio V^o/V^i, for the case $\Delta\Psi_{tm} = -50$ mV with GUVs composed of POPC/POPG/CHOL (70/10/20). For low TPP^+ concentrations, the largest difference in the inner versus outer quadrupolar splittings is predicted to occur for the case that $V^o > V^i$. The explanation is that, at low TPP^+ concentrations, in the presence of a transmembrane electrical potential (negative inside), when $V^o \leq V^i$, the TPP^+ concentration in the inner aqueous compartment can actually be limited by the absolute size of the external TPP^+ reservoir. When $V^o > V^i$, this constraint is lifted. At high TPP^+ concentrations, the maximum difference $\Delta\nu_{diff}$ is predicted to occur for the case that $V^o < V^i$. Here, the external TPP^+ reservoir is so

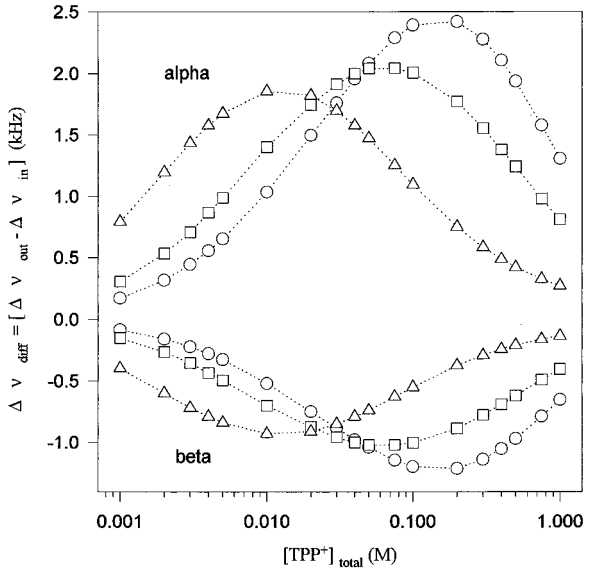

FIGURE 3: Model predictions of the effect of increasing the mole percent of POPG on the difference between the ^{2}H NMR quadrupolar splittings from the inner versus the outer monolayer, $\Delta\nu_{diff}$, for POPC-α-d_2 and POPC-β-d_2, in GUVs composed of POPC/POPG/CHOL (80 − x/x/20) and having $\Delta\Psi_{tm} = -50$ mV with $V^o/V^i = 1$: circles, 0 mol % POPG; squares, 10 mol % POPG; and triangles, 30 mol % POPG.

easily depleted that significant external TPP$^+$ binding only occurs at the highest TPP$^+$ concentrations.

Figure 3 illustrates the predicted effects of varying the mole fraction of POPG in the GUVs while maintaining the CHOL content at 20 mol %. Values of $\Delta\nu_{diff}$ are shown for the case $V^o = V^i$ and $\Delta\Psi_{tm} = -50$ mV. The addition of POPG has two major effects. First, the TPP$^+$ concentration yielding the maximum value of $\Delta\nu_{diff}$ shifts toward lower values with increasing mole fraction of POPG. Second, the maximum $\Delta\nu_{diff}$ which can be achieved decreases with increasing mole fraction of POPG. Both effects are due to the negative surface charge created initially by POPG. This attracts TPP$^+$ toward the membrane surface so that its concentration at the surface exceeds its concentration in the bulk solution, thereby enhancing binding. Consequently, TPP$^+$ binding to the inner surface saturates at a lower TPP$^+$ concentration than it would without POPG, and the TPP$^+$ binding to the outer surface is better able to "catch up".

Experimental Verification of the Model. An essential prerequisite to any test of the predictions of our model is the availability of an experimental system in which a transmembrane potential of sufficient duration can be generated that significant decay does not occur on a time scale adequate to obtain useful ^{2}H NMR spectra. Preliminary experiments using Safranin O showed that transmembrane potentials of −200 mV (negative inside) could be generated in POPC/POPG/CHOL GUVs, provided the CHOL content did not exceed 20 mol %. Higher CHOL contents presumably inhibit the transmembrane shuttling of valinomycin (de Gier et al., 1970). With the system [150 mM K_2SO_4]$_{inside}$ + [225 mM choline chloride]$_{outside}$ + (1/10^4 valinomycin/lipid), as described by de Kroon et al. (1991b), the transmembrane potential so generated was stable for at least 24 h. Parallel ^{31}P and ^{2}H NMR experiments revealed that a CHOL content of at least 20 mol % was necessary to yield GUVs of a sufficient size to avoid undesirable vesicle tumbling effects on the ^{2}H NMR spectral line shape at room temperature. Leenhouts et al. (1993) avoided this problem by acquiring ^{2}H NMR spectra only at low temperatures.

Table 1: ^{2}H NMR Quadrupolar Splittings from the Inner and Outer Monolayers of GUVs under the Influence of a Transmembrane Potential-Driven TPP$^+$ Redistribution

$\Delta\Psi_{tm}$ (mV)	[TPP$^+$] (mM)	V^o+V^i (μL)	$\Delta\nu$ POPC-α-d_2 (kHz)			$\Delta\nu$ POPC-β-d_2 (kHz)		
			$\Delta\nu_o$	$\Delta\nu_i$	$\Delta\nu_{diff}$	$\Delta\nu_o$	$\Delta\nu_i$	$\Delta\nu_{diff}$
POPC/POPG/CHOL (70/10/20)								
0	0	400	7.9	7.9	0	4.3	4.3	0
−200	0	400	7.9	7.9	0	4.3	4.3	0
−200	10	400	6.7	4.3	2.4	4.9	6.0	1.1
0	10	600	6.1	6.1	0	5.1	5.1	0
−200	2.5	600	7.7	5.6	2.1			
−200	5.0	600	7.2	5.0	2.2			
−200	10	600	6.7	3.7	3.0	5.0	6.4	1.4
−200	10	900	6.6	3.5	3.1			
−200	20	900	5.9	3.7	2.2			
−200	30	900	4.4	3.0	1.4			
POPC/POPG/CHOL (60/20/20)								
0	0	400	8.4	8.4	0	3.1	3.1	0
−200	0	400	8.4	8.4	0	3.1	3.1	0
−200	10	400	7.4	5.1	2.3	3.7	5.1	1.4
0	10	600	6.2	6.2	0	4.5	4.5	0
−200	10	600	6.8	4.2	2.6	3.8	5.6	1.8
−200	10	800				3.7	5.7	2.0
−200	20	800				4.6	6.2	1.6

Figure 4 (A and B) shows ^{2}H NMR spectra for GUVs composed of POPC/POPG/CHOL (70/10/20) and containing either POPC-α-d_2 (Figure 4A) or POPC-β-d_2 (Figure 4B). The top spectrum in both cases was acquired using GUV with $\Delta\Psi_{tm}$ equal to −200 mV and no TPP$^+$ (total volume of 600 μL). The spectral line shape is a Pake doublet, characteristic of lipids in a liquid−crystalline bilayer, undergoing rapid anisotropic motional averaging about their long molecular axes normal to the plane of the bilayer, but only slow isotropic motional averaging from the combination of overall vesicle tumbling and lateral diffusion of the lipids within the plane of the bilayer. This desirable situation is achieved when the vesicle radius exceeds 250 Å or, if the vesicles are smaller, when the measuring temperature is lowered. The quadrupolar splitting corresponds to the separation, in hertz, between the two maxima in the spectrum. The sizes of the quadrupolar splittings (see Table 1 for details) differ from the values measured in the absence of POPG in precisely the counterdirectional fashion predicted by the molecular voltmeter for the addition of 10 mol % POPG (Macdonald & Seelig, 1988). Furthermore, these quadrupolar splittings correspond closely with those obtained with POPC/POPG (90/10) MLVs (Macdonald & Seelig, 1988). It follows that the molecular voltmeter response is fully intact in GUVs and that CHOL has little if any influence on either the surface charge density or the sensitivity of the molecular voltmeter response, as shown previously (Marassi et al., 1993b). Moreover, this confirms the finding of Leenhouts et al. (1993) that the transmembrane electrical potential alone induces no apparent conformation change in the PC head group. Since only a single quadrupolar splitting is observed with either POPC-α-d_2 or POPC-β-d_2, the inner and outer bilayer surfaces of the lipid vesicle experience identical surface charge densities. We note that none of the aqueous ions present at this point (choline$^+$, Cl^-, K^+, SO_4^{2-}) bind to lipid bilayer surfaces with sufficient affinity so as to influence the ^{2}H NMR quadrupolar splittings, while valinomycin is present only at levels of 1 per 10 000 lipids.

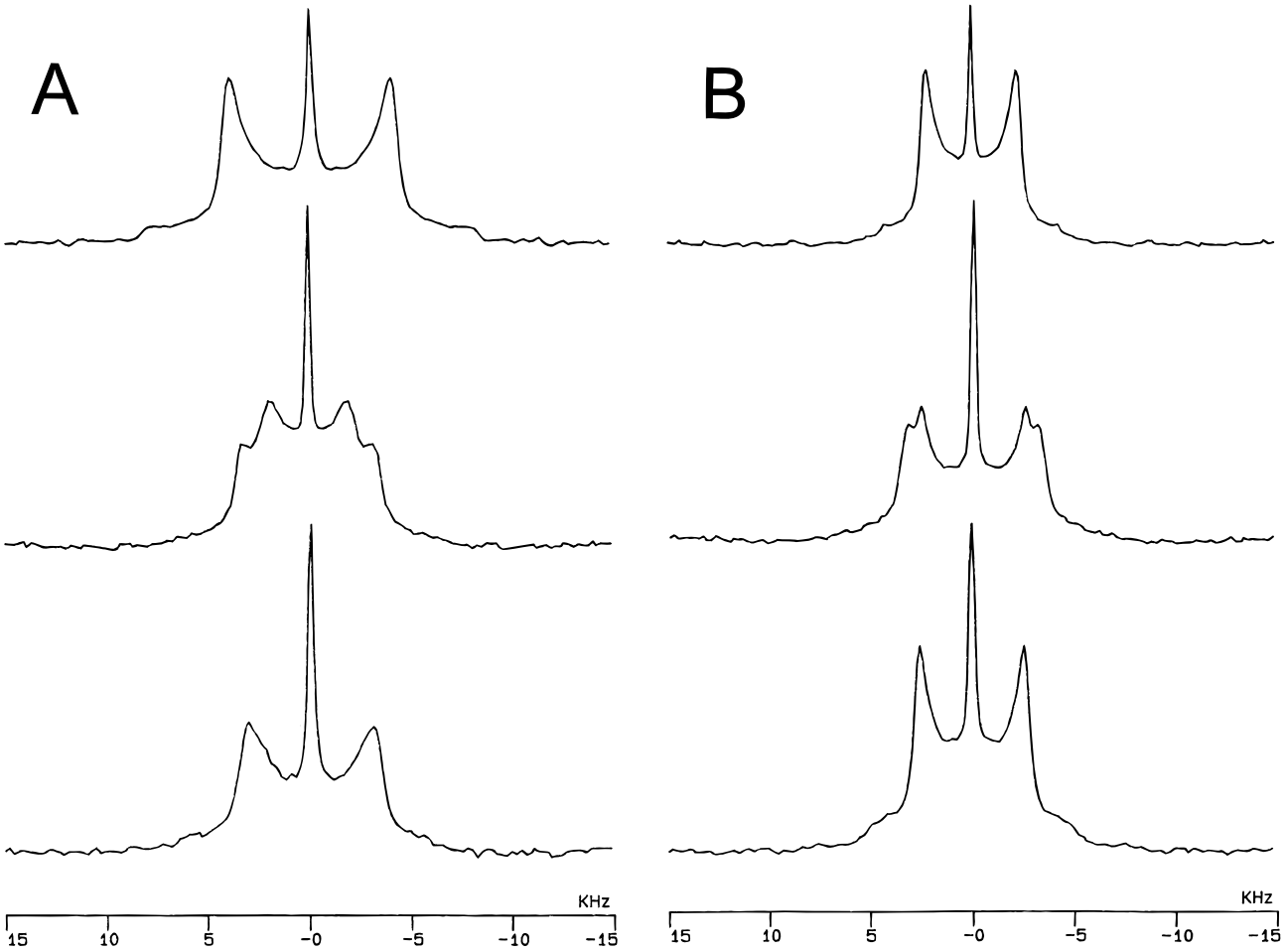

FIGURE 4: Experimental verification of the predicted effects of a transmembrane potential- driven TPP^+ redistribution on ^2H NMR quadrupolar splittings from POPC-α-d_2 and POPC-β-d_2. GUVs were composed of POPC/POPG/CHOL (70/10/20), total volume ($V^o + V^i$) = 600 uL, and $\Delta\Psi_{tm} = -200$ mV. Spectra in A were recorded with POPC-α-d_2, and spectra in B were recorded with POPC-β-d_2: top spectra, $\Delta\Psi_{tm} = -200$ mV, no TPP^+; middle spectra, $\Delta\Psi_{tm} = -200$ mV, 10 mM TPP^+; and bottom spectra, $\Delta\Psi_{tm} = 0$ mV (due to freeze−thaw), 10 mM TPP^+.

The middle ^2H NMR spectra in Figure 4A,B are obtained upon addition of 10 mM TPP^+ to POPC/POPG/CHOL (70/10/20) GUVs having $\Delta\Psi_{tm}$ equal to −200 mV (total volume of 600 μL). The spectra for both POPC-α-d_2 and POPC-β-d_2 consist of two clearly distinguished overlapping Pake doublets, indicating two discrete lipid populations experiencing different surface charge densities. For POPC-α-d_2, both quadrupolar splittings are decreased relative to the value measured in the absence of TPP^+, while for POPC-β-d_2, both quadrupolar splittings are increased relative to the value measured in the absence of TPP^+ (for details see Table 1). Therefore, in all instances, the addition of TPP^+ produces a change in the quadrupolar splittings consistent with an accumulation of cationic charges at the membrane surface due to TPP^+ binding. The different surface charge densities experienced by the two lipid populations is a consequence of the redistribution of TPP^+ into the interior of the GUVs ($\Delta\Psi_{tm}$ negative inside) resulting in a higher level of TPP^+ binding to the interior monolayer of the lipid vesicle relative to the exterior monolayer. Thus, the system responds qualitatively in the fashion predicted by the model. Quantitatively, the differences in the quadrupolar splittings for the inner versus the outer monolayer observed here ($\Delta\nu_{diff}$ = 3000 Hz for POPC-α-d_2 and $\Delta\nu_{diff}$ = 1400 Hz for POPC-β-d_2) agree with the predictions of the model for the case $\Delta\Psi_{tm} = -200$ mV and $V^o/V^i \sim 1$.

The bottom spectra in Figure 4A,B demonstrate that when $\Delta\Psi_{tm}$ is dissipated (in this case by freeze−thawing the GUVs) any differences in the surface charge at the inner versus the outer monolayer of the vesicle bilayer disappear, since only a single quadrupolar splitting is observed for either POPC-α-d_2 or POPC-β-d_2. Hence, differences in surface charge at the two monolayers of the vesicle's bilayer are entirely dependent on the presence of a transmembrane electrical potential. The size of the single resulting quadrupolar splitting is intermediate to the two values observed in the presence of a transmembrane potential. A single quadrupolar splitting of identical size is obtained if TPP^+ is simply added to the same GUVs before any addition of valinomycin.

Figure 5 (A and B) illustrates the effects of changing the proportion of the extra- to intra vesicular volume, V^o/V^i, as well as the effects of increasing the proportion of POPG in the mixed POPC/POPG/CHOL GUVs, on the resolution of the ^2H NMR quadrupolar splittings from the inner versus the outer monolayer of the vesicle bilayer. In this instance, the GUVs are composed of POPC/POPG/CHOL (80 − x/x/20) having $\Delta\Psi_{tm}$ equal to −200 mV, with 10 mM TPP^+ added in all cases. ^2H NMR spectra obtained with POPC-α-d_2 are shown in Figure 5A, while spectra obtained with POPC-β-d_2 are shown in Figure 5B.

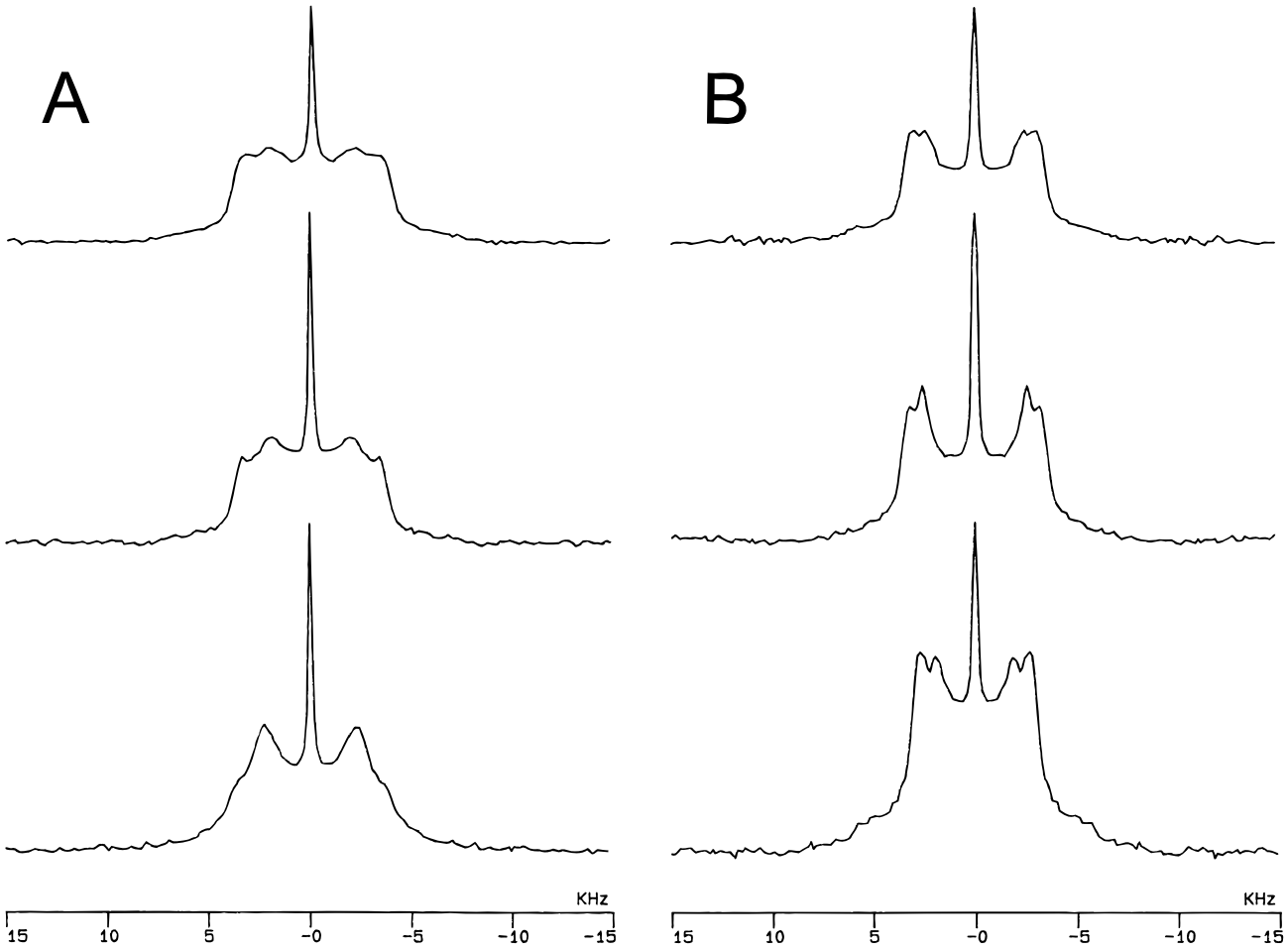

FIGURE 5: Experimental verification of the predicted effects of altering the extra- to intravesicular volume ratio, V^o/V^i, and the mol % POPG, on ^{2}H NMR quadrupolar splittings from POPC-α-d_2 and POPC-β-d_2 in the presence of a transmembrane potential-driven TPP$^+$ redistribution . Spectra in A were recorded with POPC-α-d_2, and spectra in B were recorded with POPC-β-d_2: top spectra, GUVs composed of POPC/POPG/CHOL (70/10/20), $\Delta\Psi_{tm} = -200$ mV, 10 mM TPP$^+$, total volume ($V^o + V^i$) = 400 μL; middle spectra, GUVs composed of POPC/POPG/CHOL (70/10/20), $\Delta\Psi_{tm} = -200$ mV, 10 mM TPP$^+$, total volume ($V^o + V^i$) = 600 μL; and bottom spectra, GUVs composed of POPC/POPG/CHOL (60/20/20), $\Delta\Psi_{tm} = -200$ mV, 10 mM TPP$^+$, total volume ($V^o + V^i$) = 600 μL.

The top and middle spectra were obtained when the total volume of a GUV preparation composed of POPC/POPG/CHOL (70/10/20) was increased from 400 to 600 μL by the addition of 200 μL of 10 mM TPP$^+$ (i.e. TPP$^+$ concentration remains constant). For both POPC-α-d_2 and POPC-β-d_2, an enhanced $\Delta\nu_{diff}$ is observed upon increasing V^o/V^i, in accordance with the predictions of the model for the case of 10 mM TPP$^+$ with 10 mol % POPG (details are listed in Table 1). V^i is estimated to equal approximately 300 μL for these GUV preparations, on the basis of the vesicle diameter established from light scattering and electron micoscopy studies (Marassi & Macdonald, 1993b) and assuming reasonable values for the cross sectional areas occupied by the various lipids within the bilayers as detailed earlier. Consequently, increasing the total volume of the GUVs from 400 to 600 μL corresponds to changing V^o/V^i from 1/3 to 1/1. Further incremental gains in $\Delta\nu_{diff}$ are achieved when the total volume is increased to 900 μL, as detailed in Table 1, but beyond this volume, signal-to-noise in the spectrum begins to erode seriously as the sample volume exceeds the sensitive volume of the NMR probe's sample coil. Our model predicts that, in this regime of TPP$^+$ concentrations, large gains in $\Delta\nu_{diff}$ will be achieved only when $V^o \gg V^i$. Realizing such resolution enhancements, therefore, will require specific adjustments to the NMR probe configuration.

The bottom spectra in Figure 5 A,B illustrate the effects of increasing the POPG content of the GUVs to 20 mol %. For both POPC-α-d_2 and POPC-β-d_2, an enhanced $\Delta\nu_{diff}$ is observed at higher POPG levels (see Table 1 for details), in conformity to the predictions of our model for the case of 10 mM TPP$^+$. We note, however, that for POPC-α-d_2 resolution of the two quadrupolar splittings is poor, for reasons explained below.

Experimental Factors Limiting Resolution. The mathematical model described above provides guidelines for enhancing resolution in ^{2}H NMR measurements of transmembrane potential- driven transbilayer surface charge asymmetries, the utility of which is evident in the ^{2}H NMR spectra in Figures 4 and 5. However, several experimental limitations, not explicitly accounted for in the model, result in a failure to achieve the predicted values of $\Delta\nu_{diff}$ or else an inability to resolve the quadrupolar splittings from the lipid populations at the inner and outer monolayer despite large values of $\Delta\nu_{diff}$.

One particular assumption likely to prove inadequate is that the quadrupolar splitting at any one monolayer surface is a linear function of the mole fraction of charged lipid species at that surface. In fact, the relationship between $\Delta\nu_j$

and the surface charge density is generally curvilinear (Seelig et al., 1987; Scherer & Seelig, 1989), such that with increasing surface charge density the response of the quadrupolar splittings is dampened. Incorporating this more realistic calibration of the relationship between $\Delta\nu_j$ and X_j has the effect of decreasing the maximum values of $\Delta\nu_{diff}$ and shifting the optimal TPP^+ concentrations toward lower values. Experimentally, when we titrate GUVs with increasing amounts of TPP^+ , we observe that maximum values of $\Delta\nu_{diff}$ are obtained with 10 mM TPP^+, for the case POPC/POPG/CHOL (70/10/20), $\Delta\Psi_{tm} = -200$ mV, and $V_{total} = 900\ \mu$L. Details are provided in Table 1. Note that both quadrupolar splittings continue to decrease with increasing TPP^+ concentration, so that saturation of binding is not responsible for the observed decrease in $\Delta\nu_{diff}$.

A second difficulty arises due to the nature of the ^{2}H NMR Pake doublet spectral line shape. Two equal populations of deuterons will have equal integrated areas of their corresponding Pake doublets, regardless of the actual quadrupolar splitting. If the quadrupolar splitting increases, the signal-to-noise ratio decreases at the "horns" of the spectrum, where the quadrupoloar splitting is measured. This effect is evident in Figure 5, where, for POPC-α-d_2 in POPC/POPG/CHOL (60/20/20) GUVs, the Pake doublet with the larger quadrupolar splitting is barely discernable as a distinct spectral component, although $\Delta\nu_{diff}$ is quite large in this instance. It follows that $\Delta\nu_{diff}$ is not always the best indicator of achievable resolution. In such cases, de-Paking of the experimental deuterium spectra would undoubtedly prove useful for resolving inner versus outer quadrupolar splittings (Bloom & Sternin, 1987).

Any heterogeneity in the surface charge experienced by the individual populations constitutes a further source of decreased resolution. This might arise, for example, if TPP^+ were not completely equilibrated amongst all the intravesicular volumes in the entire sample. Typically, 4 to 6 h of equilibration time after the addition of TPP^+ is required to attain the level of resolution displayed in the ^{2}H NMR spectra shown here. We expect that this is a consequence of including CHOL in the lipids of which the GUVs are composed (de Gier et al., 1970). Equilibration times do appear to be somewhat shorter when the ratio V^o/V^i increases.

SUMMARY AND CONCLUSIONS

^{2}H NMR detection of transmembrane potential-driven transbilayer surface charge asymmetries is now a practical possibility, as demonstrated here for the case of the potential-sensitive dye TPP^+. Further improvements in sensitivity and resolution will require adjustments of specific experimental and instrumental variables, none of which constitute insurmountable obstacles. A broad range of applications of this technology can now be pursued. Of particular interest and immediacy is the study of the transmembrane trafficking of charged species such as the cationic lipid−DNA complexes employed in gene transfer systems (Felgner & Rhodes, 1991) or fatty acids, fatty acid analogues, and bile acids (Kamp & Hamilton, 1993).

REFERENCES

Åkerman, K. E., & Saris, N. L. (1976) *Biochim. Biophys. Acta 426*, 624−629.

Akutsu, H., & Seelig, J. (1981) *Biochemistry 20*, 7366−7373.

Alberts, B., Bray, D., Lewis, J., Raff, M., Roberts, K., & Watson, J. (1989) *Molecular Biology of the Cell*, Garland Publishing Inc., New York.

Aloy, M. M., & Rabout, C. (1913) *Bull. Soc. Chim. Fr. 13*, 457−460.

Altenbach, C., & Seelig, J. (1984) *Biochemistry 23*, 3913−3920.

Altenbach, C., & Seelig, J. (1985) *Biochim. Biophys. Acta 818*, 410−415.

Aneja, R., Chada, J. S., & Davies, A. P. (1970) *Biochim. Biophys. Acta 218*, 102−111.

Beschiaschvili, G., & Seelig, J. (1991) *Biochim. Biophys. Acta 1061*, 78−84.

Bloom, M., & Sternin, E. (1987) *Biochemistry 26*, 2101−2105.

Boulanger, Y., Schrier, S., & Smith, I. C. P. (1981) *Biochemistry 20*, 6824−6830.

Cafiso, D. S., & Hubbell, W. L. (1978) *Biochemistry 17*, 187−195.

Catterall, W. A. (1986) *Annu. Rev. Biochem. 55*, 953−958.

Comfurius, P., & Zwaal, R. F. A. (1977) *Biochim. Biophys. Acta 488*, 36−42.

Davidson, V. L., Cramer, W. A., Bishop, L. J., & Brunden, K. R. (1984) *J. Biol. Chem. 259*, 594−600.

Davis, J. H., Jeffrey, K. R., Bloom, M., Valic, M. I., & Higgs, T. P. (1976) *Chem. Phys. Lett. 42*, 390−394.

de Gier, J., Haest, C. W. M., Mandersloot, J. G., & van Deenen, L. L. M. (1970) *Biochim. Biophys. Acta 211*, 373−376.

de Kroon, A., Killian, J. A., de Gier, J., & de Kruijff, B. (1991a) *Biochemistry 30*, 1151−1162.

de Kroon, A., Vogt, B., van't Hof, R., de Kruijff, B., & de Gier, J. (1991b) *Biophys. J. 60*, 525−537.

Dempsey, C., Bitbol, M., & Watts, A. (1989) *Biochemistry 28*, 6590−6596.

Felgner, P. L., & Rhodes, G. (1991) *Nature 349*, 351.

Harbisson, G. S., & Griffin, R. G. (1984) *J. Lipid Res. 25*, 1140−1142.

Kamp, F., & Hamilton, J. A. (1993) *Biochemistry 32*, 11074−11086.

Ketterer, B., Neumcke, B., & Lauger, P. (1971) *J. Membr. Biol. 5*, 225−245.

Kuchinka, E., & Seelig, J. (1989) *Biochemistry 28*, 4216−4221.

Lau, B., & Macdonald, P. M. (1995) *Biochim. Biophys. Acta 1237*, 37−42.

Leenhouts, J. M., Chupin, V., de Gier, J., & de Kruijff, B. (1993) *Biochim. Biophys. Acta 1153*, 257−261.

Macdonald, P. M., & Seelig, J. (1988) *Biochemistry 27*, 6769−6775.

Macdonald, P. M., Liesen, J., & Marassi, F. M. (1991) *Biochemistry 30*, 3558−3566.

Marassi, F. M., & Macdonald, P. M. (1991) *Biochemistry 30*, 10558−10566.

Marassi, F. M., & Macdonald, P. M. (1992) *Biochemistry 31*, 10031−10036.

Marassi, F. M., Djukic, S., & Macdonald, P. M. (1993a) *Biochemistry 32*, 219−228.

Marassi, F. M., Shivers, R. R., & Macdonald, P. M. (1993b) *Biochemistry 32*, 9936−9943.

Rottenberg, H. (1984) *J. Membr. Biol. 81*, 127−138.

Roux, M., & Bloom, M. (1990) *Biochemistry 29*, 7077−7089.

Roux, M., Neumann, J., Hodges, R. S., Devaux, P., & Bloom, M. (1989) *Biochemistry 28*, 2313−2321.

Rydall, J., & Macdonald, P. M. (1992) *Biochemistry 31*, 1092−1099.

Scherer, P. G., & Seelig, J. (1989) *Biochemistry 28*, 7720−7728.

Seelig, A., Allegrini, P. R., & Seelig, J. (1988) *Biochim. Biophys. Acta 939*, 267−276.

Seelig, J., Macdonald, P. M., & Scherer, P. G. (1987) *Biochemistry 26*, 7535−7541.

Sixl, F., & Watts, A. (1983) *Proc. Natl. Acad. Sci. U.S.A. 80*, 1613−1615.

Watts, A., & Poile, T. W. (1986) *Biochim. Biophys. Acta 861*, 368−372.

Yeagle, P. (1988) *Biology of Cholesterol*, CRC Press, Boca Raton, FL.

BI951214+